



中国科学院高能物理研究所
Institute of High Energy Physics
Chinese Academy of Sciences



Search for Higgs boson pair production in $\gamma\gamma b\bar{b}$ final state in pp collisions at $\sqrt{s} = 13$ TeV with the ATLAS detector

Zihang Jia^{1,2}

¹IHEP, ²Nanjing University

Outline

- **Motivation**
- **Analysis overview**
- **Categorization**
- **Signal and background modeling**
- **Results**
- **Summary**

[ATLAS-CONF-2021-016](#) (this talk)

[JHEP 11 \(2018\) 040](#) (ATLAS 36 fb^{-1})

[JHEP 03 \(2021\) 257](#) (CMS)

[ATLAS-PHYS-PUB-2021-031](#) (HH summary)

Motivation – HH production

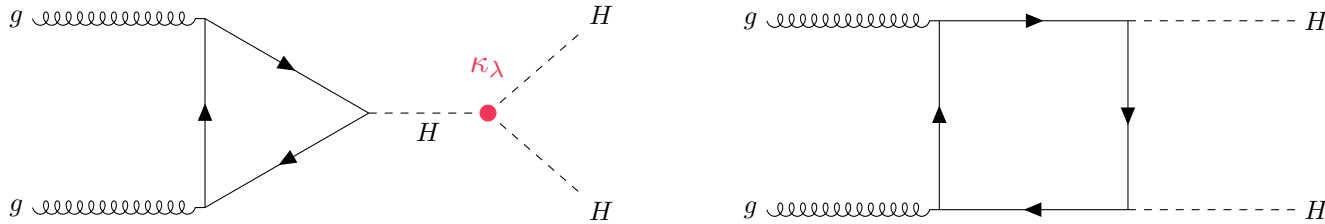
- Measuring HH production gives us access to the **trilinear Higgs self-coupling** (λ_{HHH}).

$$\kappa_\lambda = \frac{\lambda_{HHH}}{\lambda_{HHH}^{SM}}$$

SM LHCHWGHH

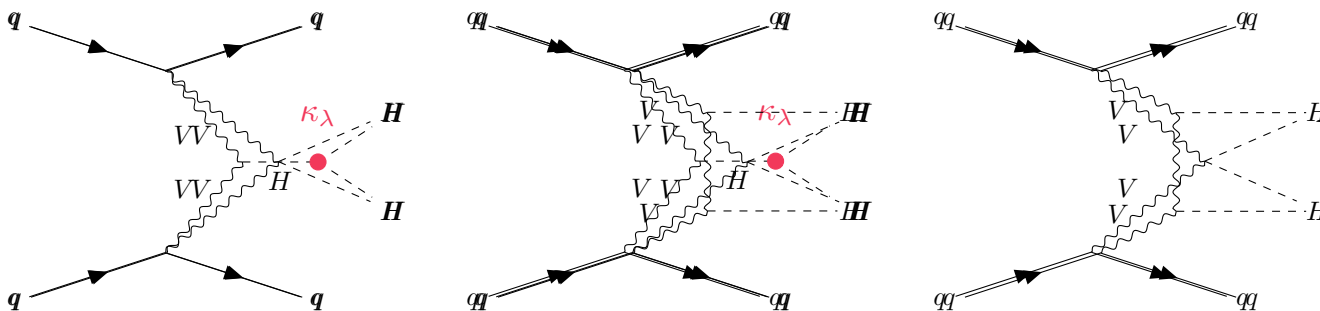
Gluon-gluon fusion (ggFHH)

- $\sigma_{NNLO} = 31.02$ [fb] @13 TeV, $m_H = 125.09$ GeV



Vector boson fusion (VBFHH)

- $\sigma_{N3LO} = 1.723$ [fb] @13 TeV, $m_H = 125.09$ GeV



BSM enhancement

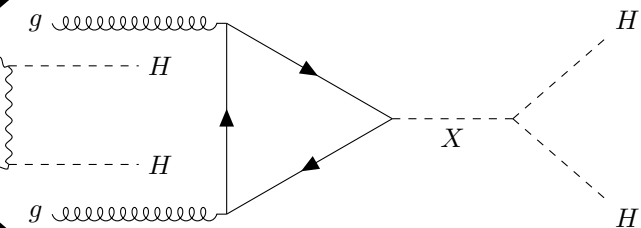
Non-resonant HH production

- Anomalous couplings ($\kappa_\lambda \neq 1$, etc.)

Resonant HH production

- Two Higgs Doublet Model

X: a narrow-width scalar particle



HH $\gamma\gamma$ Analysis overview

Search for **Non-resonant** and **Resonant** HH production in $\gamma\gamma bb$ channel (full Run2 data, 139 fb^{-1}).

One of the most sensitive HH final states:

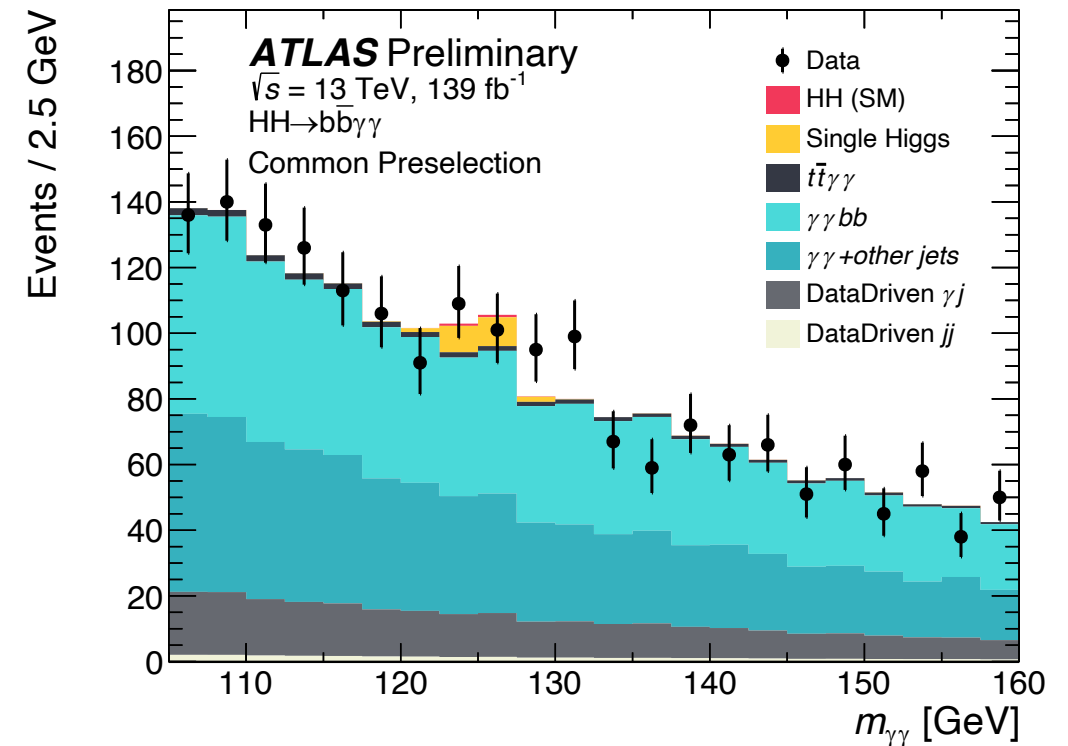
- Large branching ratio for $H \rightarrow bb$
- Excellent photon resolution and relatively small background for $H \rightarrow \gamma\gamma$

Main backgrounds

- Non-resonant $\gamma\gamma$ backgrounds
- Single Higgs production

Common Preselection

- Triggered by the presence of 2 photons
- $105 \text{ GeV} < m_{\gamma\gamma} < 160 \text{ GeV}$
- Fewer than 6 central jets (reject ttH events)
- Exactly 2 b-tagged jets (77% DL1r b-tagging efficiency)
- Veto events containing an electron or muon



Categorization

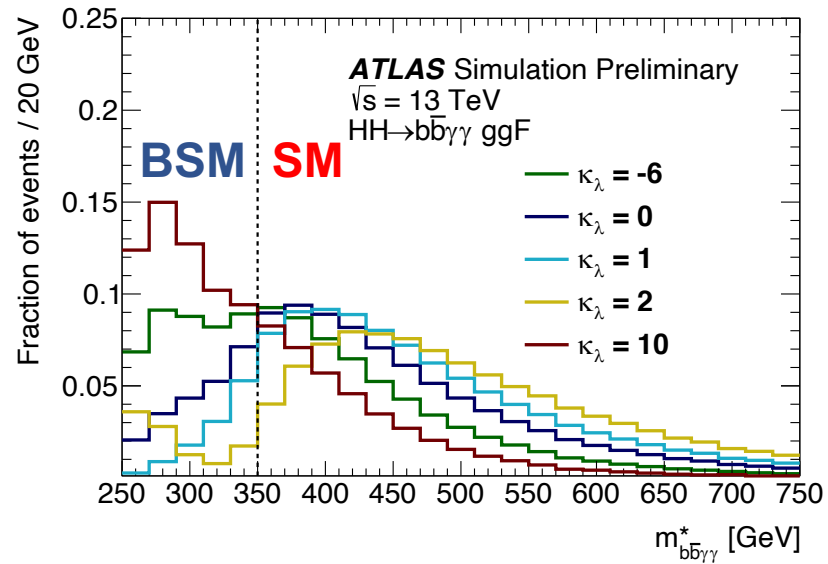
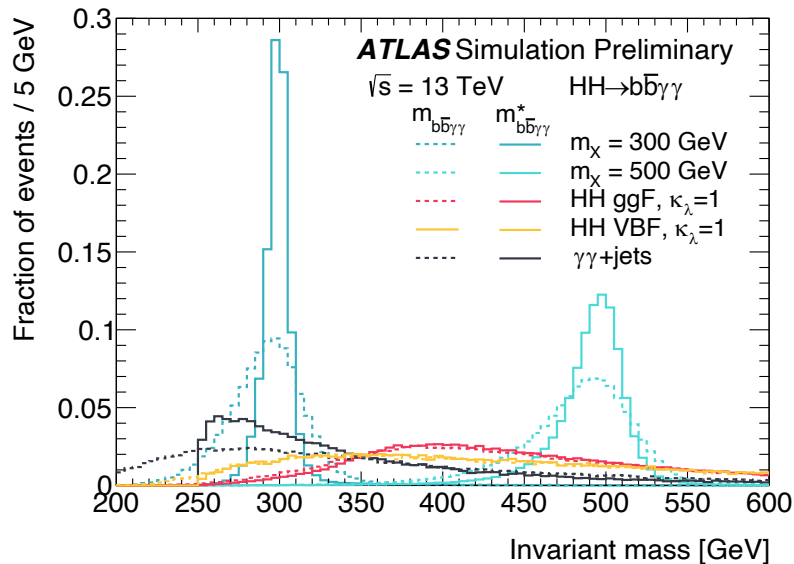
Non-resonant analysis: target SM $HH \rightarrow \gamma\gamma bb$ processes, and possible modifications to κ_λ .

Target mainly ggF HH production, but VBF HH events also considered as signal

Signal regions defined using $m_{\gamma\gamma bb}^*$ and BDT score

➤ **Modified invariant mass $m_{\gamma\gamma bb}^* = m_{\gamma\gamma bb} - m_{\gamma\gamma} - m_{bb} + 250 \text{ GeV}$**

- Provides cancellation of experimental resolution effects
- **Low** and **high** mass categories provide enhanced sensitivity to κ_λ



**Low mass region
Targeting BSM**

$m_{\gamma\gamma bb}^* < 350 \text{ GeV}$

**High mass region
Targeting SM**

$m_{\gamma\gamma bb}^* > 350 \text{ GeV}$

Categorization

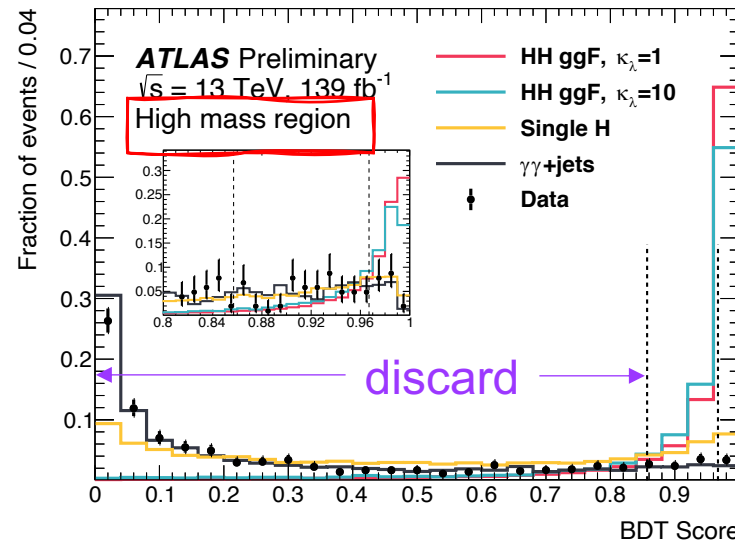
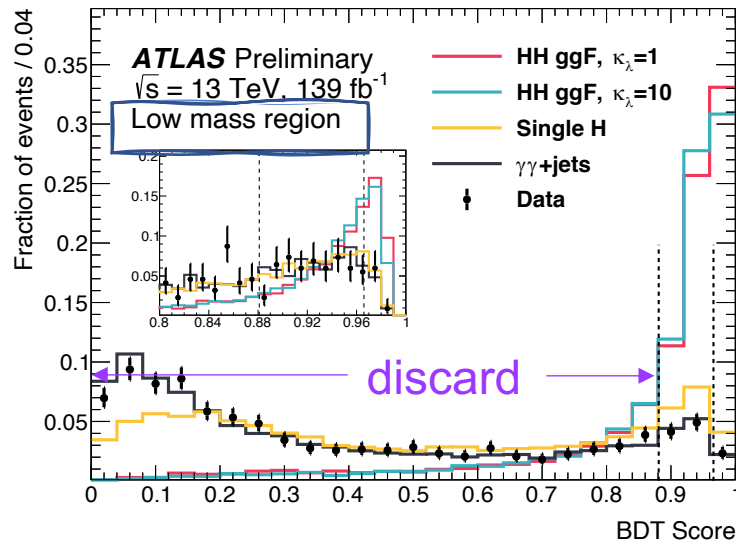
Non-resonant analysis: target SM $HH \rightarrow \gamma\gamma bb$ processes, and possible modifications to κ_λ .

Target mainly ggF HH production, but VBF HH events also considered as signal

Signal regions defined using $m_{\gamma\gamma bb}^*$ and BDT score

➤ Boosted Decision Tree

- Against $\gamma\gamma$ and single Higgs backgrounds
- BDT trained on photon, jet and missing transverse energy variables



Low mass region
Signal: $\kappa_\lambda = 10$ ggF HH

Loose
Tight

High mass region
Signal: $\kappa_\lambda = 1$ ggF HH

Loose
Tight

Categorization

Resonant analysis: target BSM $HH \rightarrow X \rightarrow \gamma\gamma bb$ processes, with $m_X \in [251, 1000]$ GeV.

Non-resonant SM HH production included as background

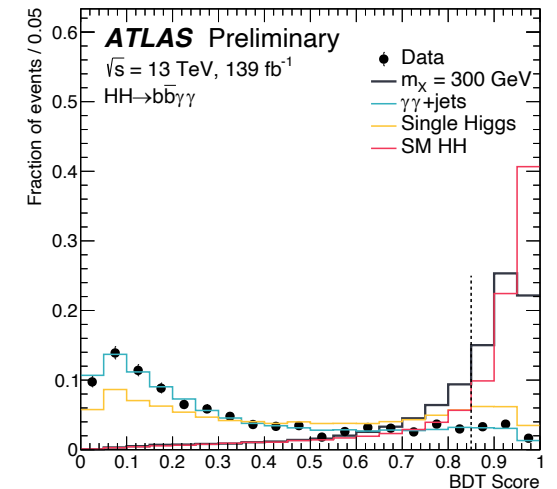
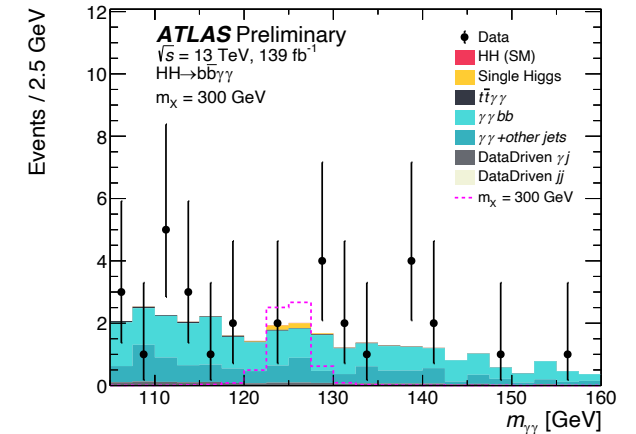
Signal regions defined using $m_{\gamma\gamma}^*$ and BDT score

➤ **Modified invariant mass**

- 2σ window cut around each mass hypothesis of the resonance

➤ **Boosted Decision Tree**

- Shared by all resonance masses to avoid lack of background at high mass
- BDTs trained on photon, jet and missing transverse energy variables
- Two BDTs against $\gamma\gamma+tt\gamma\gamma$ and single Higgs backgrounds respectively
- For each m_X , cut on the combined BDT score.



Signal and background modeling

Maximum likelihood fit performed on $m_{\gamma\gamma}$ simultaneously with all the categories.

(**Non-resonant**: 4 categories; **Resonant**: 1 category for each m_X)

➤ Signal parameterization

Normalization fixed to SM, shape from a **double sided crystal ball (DSCB)** fit to MC

Non-resonant

- Fit to SM HH signal, model shared with H background

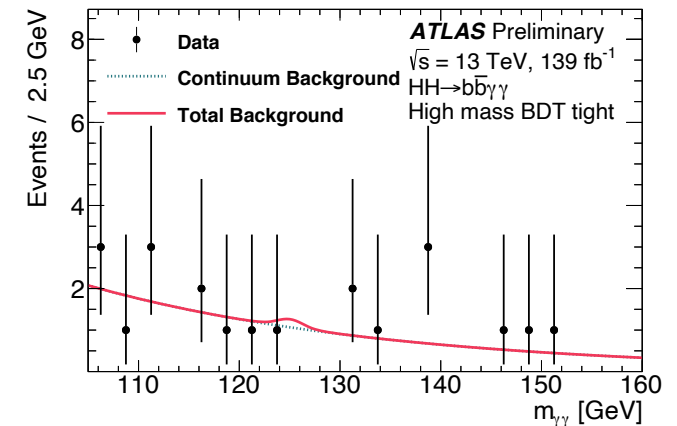
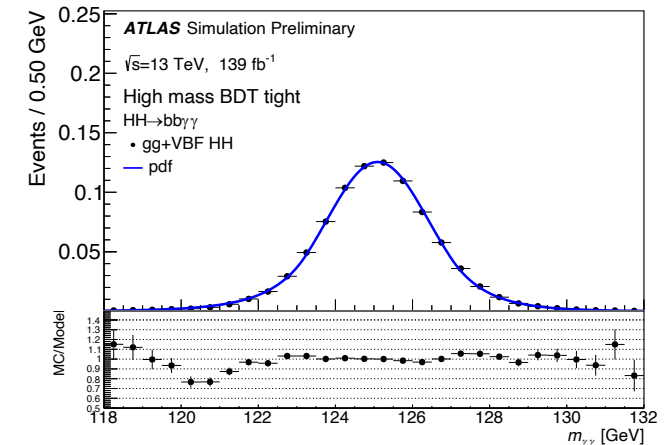
Resonant

- Fit to resonance signals, model shared with SM HH and H background

➤ Background parameterization

Normalization floating, shape from a **exponential function** fit to data

- Function form determined from **spurious signal** studies



Observed (Expected) Results

Limits at 95%CL are set based on the profile likelihood ratio approach.

Non-resonant

- μ_{HH} limit: 4.1 x SM (5.5 x SM)
- κ_λ interval: [-1.5, 6.7] ([-2.4, 7.7])

~ 5 improvement w.r.t 36 fb^{-1}
 ~2 from increase of lumi
 ~2.5 from analysis strategy

Shrinks by a factor of ~2

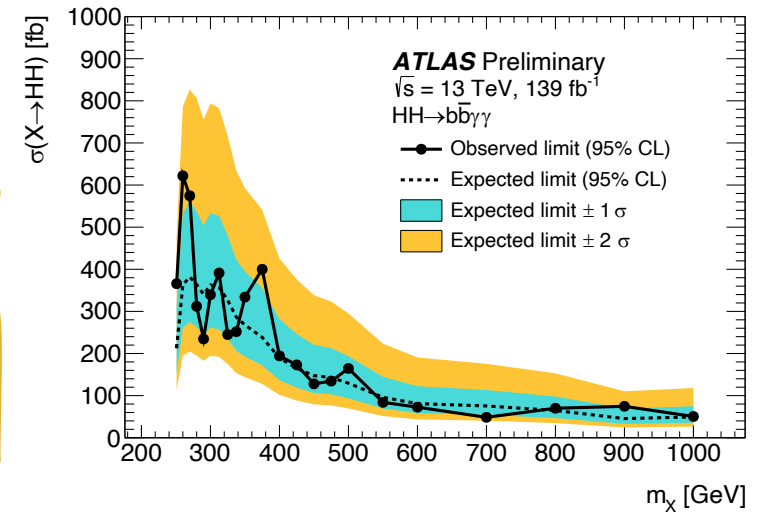
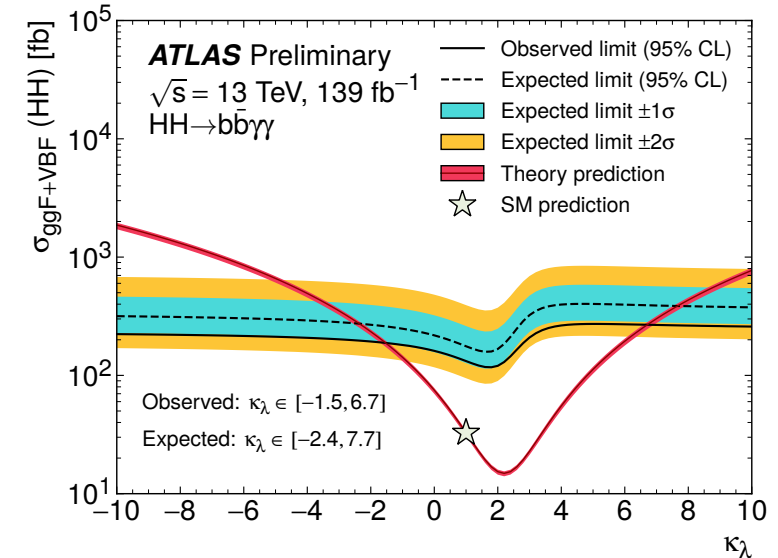
ATLAS 36 fb^{-1} JHEP 11 (2018) 040
 μ_{HH} limit: 22 (28) x SM
 κ_λ interval: [-8.2, 13.2] ([-8.3, 13.2])

CMS JHEP 03 (2021) 257
 μ_{HH} limit: 7.7 (5.2) x SM
 κ_λ interval: [-3.3, 8.5] ([-2.5, 8.2])

Resonant

- XS limits vary between 610-47 fb (360-43 fb)

~2-3 improvement depending on the m_X value
 ~2 from increase of lumi; ~1.2 from analysis strategy
 Expands the analyzed mass range of the resonance search to lower values.



Summary

Searches for **non-resonant** and **resonant** HH production are performed in the $bb\gamma\gamma$ final state (139 fb^{-1}).

No significant excess with respect to the SM background expectation is observed.

Improvement compared to the previous ATLAS result based on 36 fb^{-1} of 13 TeV pp collisions

- Extends the data set by more than a factor of 4
- Incorporates a categorization based on $m_{\gamma\gamma bb}^*$ and multivariate event selections
- More precise object reconstruction and calibration

Publication of the Run 2 paper soon.

Preparing the dedicated analysis for VBFHH signal.



中国科学院高能物理研究所
Institute of High Energy Physics
Chinese Academy of Sciences



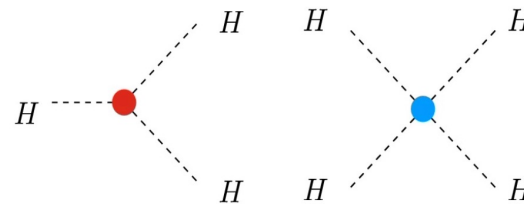
Thanks!

Motivation – Higgs self-coupling

- **The Higgs boson** completes the Standard Model of Particle Physics.
- However, the shape of **the Higgs potential** has yet to be measured.
- We can probe the Higgs potential by measuring the **Higgs self-coupling (λ)**.

$$V(\phi) = -\mu^2\phi^2 + \lambda\phi^4$$

$$V(\nu + h) = V_0 + \frac{1}{2}m_h^2h^2 + \lambda\nu h^3 + \lambda h^4 + \dots$$



$$\kappa_\lambda = \frac{\lambda_{HHH}}{\lambda_{HHH}^{SM}}$$

Background Samples

Table 1: Summary of single Higgs boson background samples, split by production modes, and continuum background samples. The generator used in the simulation, the PDF set, and tuned parameters (tune) are also provided.

Process	Generator	PDF set	Showering	Tune
ggF	NNLOPS [65–67] [68, 69]	PDFLHC [42]	PYTHIA 8.2 [70]	AZNLO [71]
VBF	POWHEG BOX v2 [39, 66, 72–78]	PDFLHC	PYTHIA 8.2	AZNLO
WH	POWHEG BOX v2	PDFLHC	PYTHIA 8.2	AZNLO
$qq \rightarrow ZH$	POWHEG BOX v2	PDFLHC	PYTHIA 8.2	AZNLO
$gg \rightarrow ZH$	POWHEG BOX v2	PDFLHC	PYTHIA 8.2	AZNLO
$t\bar{t}H$	POWHEG BOX v2 [73–75, 78, 79]	NNPDF3.0nlo [80]	PYTHIA 8.2	A14 [81]
bbH	POWHEG BOX v2	NNPDF3.0nlo	PYTHIA 8.2	A14
$tHqj$	MADGRAPH5_aMC@NLO	NNPDF3.0nlo	PYTHIA 8.2	A14
tHW	MADGRAPH5_aMC@NLO	NNPDF3.0nlo	PYTHIA 8.2	A14
$\gamma\gamma+jets$	SHERPA v2.2.4 [56]	NNPDF3.0nlo	SHERPA v2.2.4	–
$t\bar{t}\gamma\gamma$	MADGRAPH5_aMC@NLO	NNPDF2.3lo	PYTHIA 8.2	–

Common selections

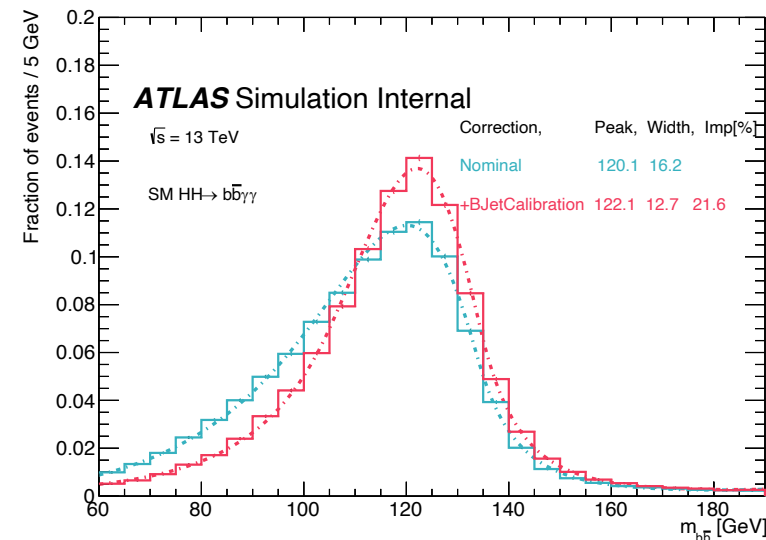
On top of the trigger requirements, events are selected if:

- there are at least two photons passing the object selection criteria detailed in Section 4.1;
- the di-photon invariant mass, built with the two leading photons, satisfies $105 \text{ GeV} < m_{\gamma\gamma} < 160 \text{ GeV}$;
- the leading (sub-leading) photon p_T is larger than 35% (25%) of the mass of the di-photon system;
- there are exactly two b -tagged jets;
- no electrons or muons are present;
- fewer than six central ($|\eta| < 2.5$) jets are required, to help rejecting $t\bar{t}H$ events where the top quarks decay hadronically.

- $p_T^{\gamma 1} > 35 \text{ GeV}$, $p_T^{\gamma 2} > 25 \text{ GeV}$
- Photon Tight ID, FixedCutLoose
- $105 < m_{\gamma\gamma} < 160 \text{ GeV}$
- $p_T^{\gamma 1}/m_{\gamma\gamma} > 0.35$, $p_T^{\gamma 2}/m_{\gamma\gamma} > 0.25$
- $N_{\text{photon}} \geq 2$
- $N_{b77 \text{ jets}} = 2$
- $N_{\text{lepton}} = 0$
- $N_{\text{central jets}} < 6$

H($b\bar{b}$)

- PFlow jets (AntiKt4PFlowCustomVtxHggJets) with $p_T > 25 \text{ GeV}$ and $|\eta| < 2.5$ passing JetVertexFraction (JVT) tight and Jet cleaning
- Exactly 2 b -jets passing the 77% DL1r b -tagging WP and ranked by p_T
 $m_{b\bar{b}}$ resolution improved by a muon-in-jet correction, as well as a p_T -reco correction to account for p_T loss due to neutrinos and objects outside of the jet cone.
 - **Resolution improves by about 22%**



Non-resonant BDT variables

Table 2: Variables used in the BDT for the non-resonant analysis. The b -tag status identifies the highest fixed b -tag working point (60%, 70%, 77%) that the jet passes. All vectors in the event are rotated so that the leading photon ϕ is equal to zero.

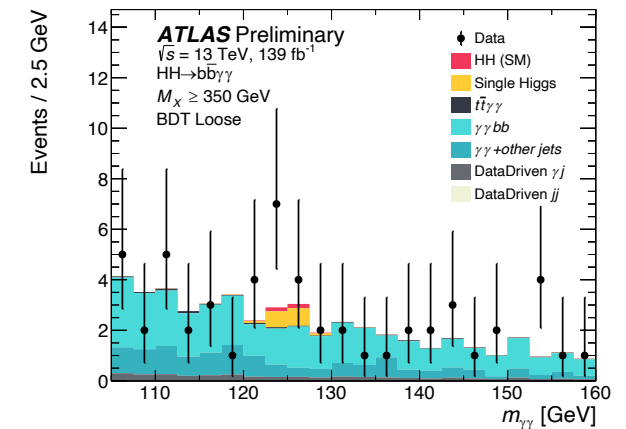
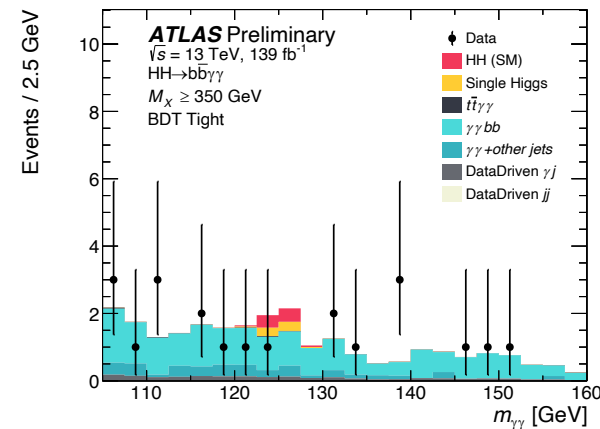
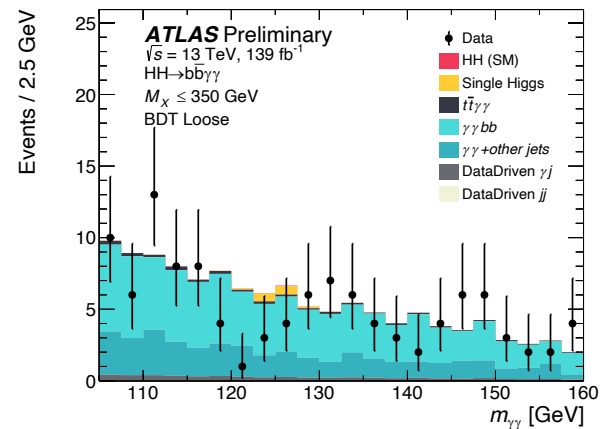
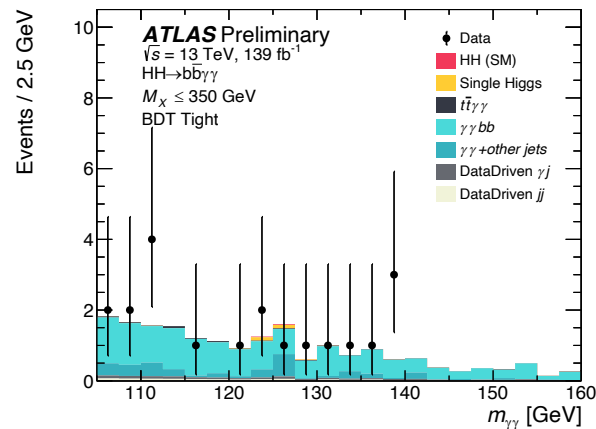
Variable	Definition
Photon-related kinematic variables	
$p_T/m_{\gamma\gamma}$	Transverse momentum of the two photons scaled by their invariant mass $m_{\gamma\gamma}$
η and ϕ	Pseudo-rapidity and azimuthal angle of the leading and sub-leading photon
Jet-related kinematic variables	
b -tag status	Highest fixed b -tag working point that the jet passes
p_T, η and ϕ	Transverse momentum, pseudo-rapidity and azimuthal angle of the two jets with the highest b -tagging score
$p_T^{b\bar{b}}, \eta_{b\bar{b}}$ and $\phi_{b\bar{b}}$	Transverse momentum, pseudo-rapidity and azimuthal angle of b -tagged jets system
$m_{b\bar{b}}$	Invariant mass built with the two jets with the highest b -tagging score
H_T	Scalar sum of the p_T of the jets in the event
Single topness	For the definition, see Eq. (1)
Missing transverse momentum-related variables	
E_T^{miss} and ϕ^{miss}	Missing transverse momentum and its azimuthal angle

Categorization

$$Z = \sqrt{2 * [(s + b) * \log(1 + s/b) - s]}$$

Low mass region

High mass region



Resonant BDT variables

Table 4: Variables used in the BDT for the resonant analysis. For variables depending on b -tagged jets, only jets b -tagged using the 77% working point are considered as described in Section 4.1.

Variable	Definition
Photon-related kinematic variables	
$p_T^{\gamma\gamma}, y^{\gamma\gamma}$	Transverse momentum and rapidity of the di-photon system
$\Delta\phi_{\gamma\gamma}$ and $\Delta R_{\gamma\gamma}$	Azimuthal angular distance and ΔR between the two photons
Jet-related kinematic variables	
$m_{b\bar{b}}, p_T^{b\bar{b}}$ and $y_{b\bar{b}}$	Invariant mass, transverse momentum and rapidity of the b -tagged jets system
$\Delta\phi_{b\bar{b}}$ and $\Delta R_{b\bar{b}}$	Azimuthal angular distance and ΔR between the two b -tagged jets
N_{jets} and $N_{b\text{-jets}}$	Number of jets and number of b -tagged jets
H_T	Scalar sum of the p_T of the jets in the event
Photons and jets-related kinematic variables	
$m_{b\bar{b}\gamma\gamma}$	Invariant mass built with the di-photon and b -tagged jets system
$\Delta y_{\gamma\gamma, b\bar{b}}, \Delta\phi_{\gamma\gamma, b\bar{b}}$ and $\Delta R_{\gamma\gamma, b\bar{b}}$	Distance in rapidity, azimuthal angle and ΔR between the di-photon and the b -tagged jets system

$$\text{BDT}_{\text{tot}} = \frac{1}{\sqrt{C_1^2 + C_2^2}} \sqrt{C_1^2 \left(\frac{\text{BDT}_{\gamma\gamma} + 1}{2} \right)^2 + C_2^2 \left(\frac{\text{BDT}_{\text{Single}H} + 1}{2} \right)^2}$$

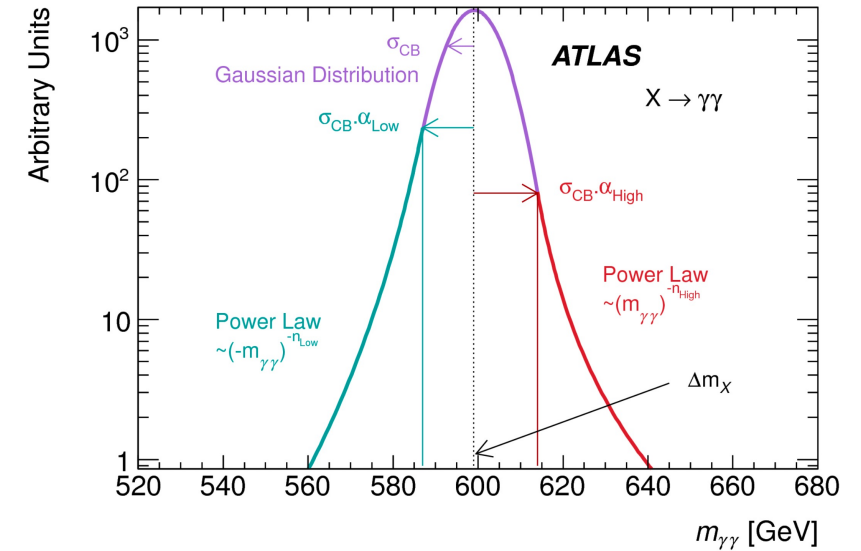
Signal modeling - DSCB

A Gaussian core + asymmetric power law tails

$$f_{\text{DSCB}}(m_{\gamma\gamma}) = N \times \begin{cases} e^{-t^2/2} & \text{if } -\alpha_{\text{low}} \leq t \leq \alpha_{\text{high}} \\ \frac{e^{-\frac{1}{2}\alpha_{\text{low}}^2}}{\left[\frac{1}{R_{\text{low}}}(R_{\text{low}} - \alpha_{\text{low}} - t)\right]^{n_{\text{low}}}} & \text{if } t < -\alpha_{\text{low}} \\ \frac{e^{-\frac{1}{2}\alpha_{\text{high}}^2}}{\left[\frac{1}{R_{\text{high}}}(R_{\text{high}} - \alpha_{\text{high}} + t)\right]^{n_{\text{high}}}} & \text{if } t > \alpha_{\text{high}} \end{cases}$$

where N is a normalization factor and the six parameters are

- μ_{CB} and σ_{CB} describe the mean and the width of the Gaussian core, which are combined in $t = (m_{\gamma\gamma} - \mu_{\text{CB}}) / \sigma_{\text{CB}}$;
- α_{low} and α_{high} are the positions of the transitions with respect to μ_{CB} from the Gaussian core to power-law tails, in unit of σ_{CB} , on the low and high mass sides respectively;
- n_{low} and n_{high} are the exponents of the low and high mass tails. With the α 's, they define $R_{\text{low}} = \frac{n_{\text{low}}}{\alpha_{\text{low}}}$ and R_{high} similarly.



Diphoton background decomposition

Reconstructed $\gamma\gamma$ events is mainly composed of $\gamma\gamma$, γ -jets and jet-jet events, where the jet(s) fake(s) a real photon. The 2x2D sideband method is developed using the discriminating power of photon identification and isolation criteria. The event yields in the signal region and the 15 sidebands can be expressed as **functions** of the photon efficiencies, jet fake rates and correlation coefficients.

Photon tight ID	Photon loose ID	C	D
	Photon tight ID	A	B
		Photon isolated	Photon non-isolated

Leading object

Photon tight ID	Photon loose ID	C	D
	Photon tight ID	A	B
		Photon isolated	Photon non-isolated

Sub-leading object

CC	CD	DC	DD
CA	CB	DA	DB
AC	AD	BC	BD
AA	AB	BA	BB

[Reference](#)

Suffers from low statistics, not used in constructing the background templates for the spurious signal procedure.

Spurious signal

Spurious signal: bias estimated from a signal + background fit to a background-only MC template.

$$N_{sp} = \max_{121 < m_H < 129 \text{ GeV}} |N_s(m_H)|$$

➤ **Selection criteria:**

❑ The function should satisfy at least one of the following criteria:

Nominal criteria

$$\begin{aligned} & N_{sp} < 10\% N_{s,exp} \\ \text{or} \\ & N_{sp} < 20\% \sigma_{bkg} \end{aligned}$$

- $N_{s,exp}$ = expected SM signal events
- σ_{bkg} = stat. uncertainty on Nsig when fitting the sig+bkg model to the asimov dataset
- Δ_{MC} = local statistical fluctuation of the MC background template

Relaxed criteria (for low-statistic bkg MC)

$$N_{sp} = \zeta_s(m_{\gamma\gamma}) = \begin{cases} N_s + 2\Delta_{MC}, & N_s + 2\Delta_{MC} < 0 \\ N_s - 2\Delta_{MC}, & N_s - 2\Delta_{MC} > 0 \\ 0, & \text{otherwise} \end{cases}$$

❑ The function must satisfy a simple χ^2 requirement in a background-only fit to the MC template:

$$p - \text{value}(\chi^2) > 1\%$$

The χ^2 is computed with a background template uniformly binned over $105 < m_{\gamma\gamma} < 160$ GeV.

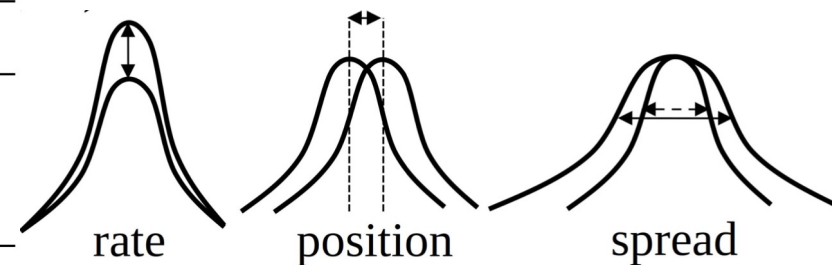
- **The least number of parameters** is preferred.
- The **smaller systematic uncertainty** (spurious signal) is preferred.

Wald tests show that the data do not prefer a higher degree functional form with respect to the exponential form.

Systematic uncertainties

In general the analysis is almost completely statistically dominated with the Run 2 dataset

Source	Type	Relative impact of the systematic uncertainties in %	
		Non-resonant analysis <i>HH</i>	Resonant analysis $m_X = 300$ GeV
Experimental			
Photon energy scale	Norm. + Shape	5.2	2.7
Photon energy resolution	Norm. + Shape	1.8	1.6
Flavor tagging	Normalization	0.5	< 0.5
Theoretical			
Heavy flavor content	Normalization	1.5	< 0.5
Higgs boson mass	Norm. + Shape	1.8	< 0.5
PDF+ α_s	Normalization	0.7	< 0.5
Spurious signal	Normalization	5.5	5.4



Statistical model

Likelihood

$$\mathcal{L} = \prod_c \left(\text{Pois}(n_c | N_c(\boldsymbol{\theta})) \cdot \prod_{i=1}^{n_c} f_c(m_{\gamma\gamma}^i, \boldsymbol{\theta}) \cdot G(\boldsymbol{\theta}) \right)$$

Event parameterization

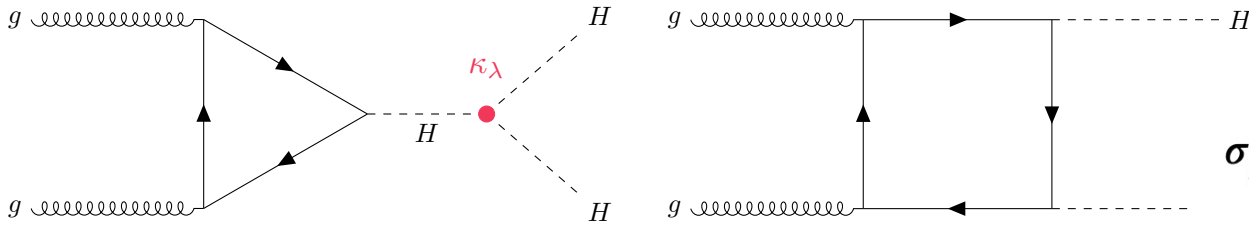
$$N_c(\boldsymbol{\theta}) = \mu \cdot N_{HH,c}(\boldsymbol{\theta}_{HH}^{\text{yield}}) + N_{\text{bkg},c}^{\text{res}}(\boldsymbol{\theta}_{\text{res}}^{\text{yield}}) + N_{\text{SS},c} \cdot \boldsymbol{\theta}^{\text{SS},c} + N_{\text{bkg},c}^{\text{non-res}}$$

Model PDF

$$f_c(m_{\gamma\gamma}, \boldsymbol{\theta}) = [\mu \cdot N_{HH,c}(\boldsymbol{\theta}_{HH}^{\text{yield}}) \cdot f_{HH,c}(m_{\gamma\gamma}, \boldsymbol{\theta}_{HH}^{\text{shape}}) + N_{\text{bkg},c}^{\text{res}}(\boldsymbol{\theta}_{\text{res}}^{\text{yield}}) \cdot f_{\text{bkg},c}^{\text{res}}(m_{\gamma\gamma}, \boldsymbol{\theta}_{\text{res}}^{\text{shape}}) + N_{\text{SS},c} \cdot \boldsymbol{\theta}_{HH}^{\text{SS},c} \cdot f_{HH,c}(m_{\gamma\gamma}, \boldsymbol{\theta}_{HH}^{\text{shape}}) + N_{\text{bkg},c}^{\text{non-res}} \cdot f_{\text{bkg},c}^{\text{non-res}}(m_{\gamma\gamma}, \boldsymbol{\theta}_{\text{non-res}}^{\text{shape}})] / N_c(\boldsymbol{\theta}_{\text{non-res}}^{\text{yield}})$$

κ_λ reweighting for ggF HH samples

The method derives the scale factors as a function of κ_λ in **bins of m_{HH}** by performing a linear combination of samples generated at $\kappa_\lambda = 0, 1, 20$.



$$\mathcal{A}(\kappa_t, \kappa_\lambda) = \kappa_t^2 \mathcal{A}_1 + \kappa_t \kappa_\lambda \mathcal{A}_2$$

$$\sigma_{\text{ggF}}(pp \rightarrow HH) \propto \int \kappa_t^4 \left[|\mathcal{A}_1|^2 + 2 \left(\frac{\kappa_\lambda}{\kappa_t} \right) \Re(\mathcal{A}_1^* \mathcal{A}_2) + \left(\frac{\kappa_\lambda}{\kappa_t} \right)^2 |\mathcal{A}_2|^2 \right]$$

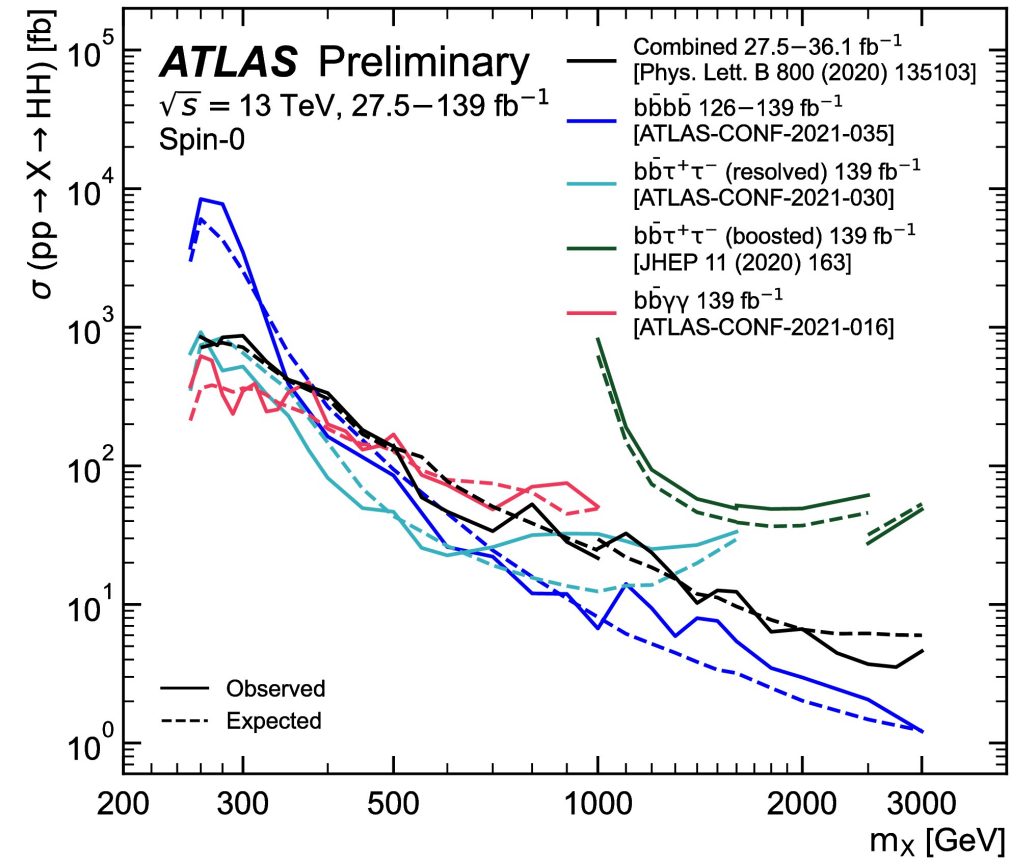
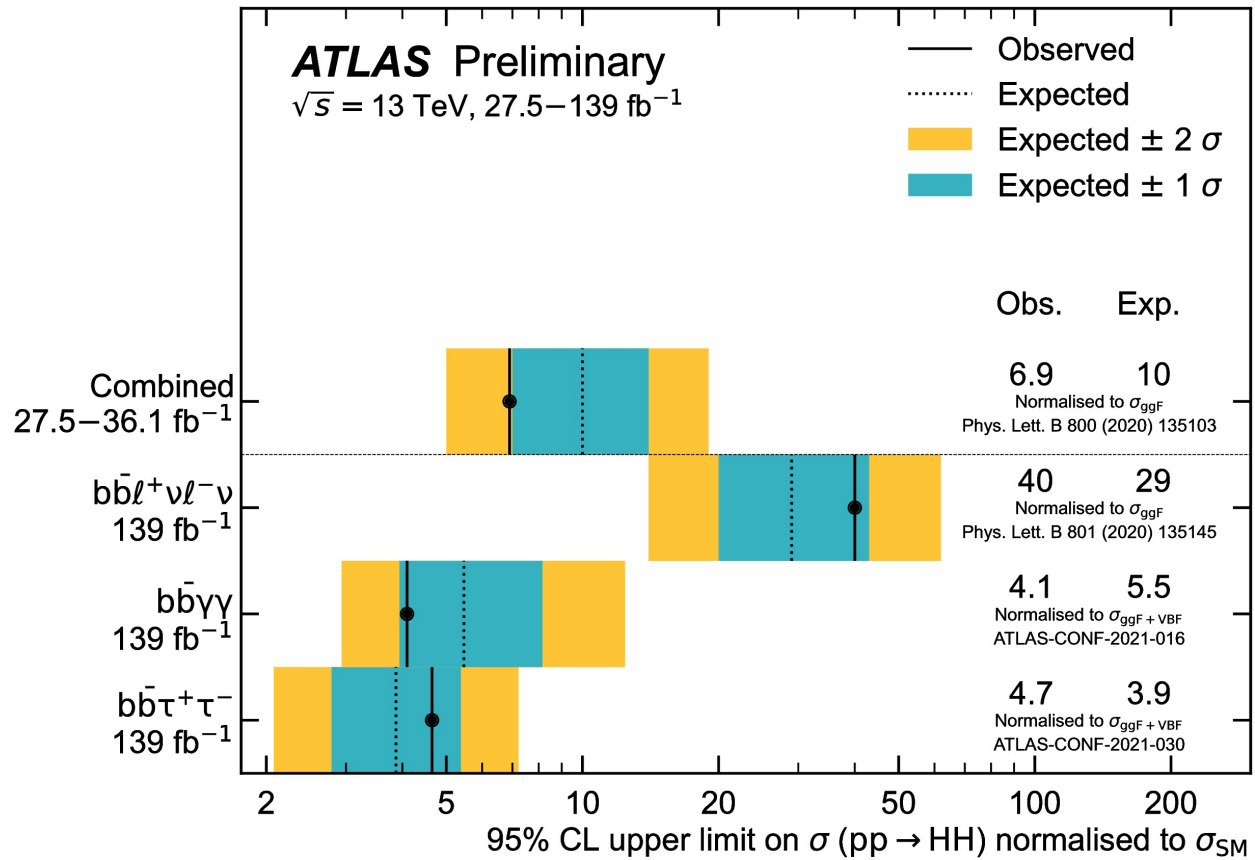
$$\sigma(\kappa_t = 1, \kappa_\lambda = 0) \sim |\mathcal{A}_1|^2$$

$$\sigma(\kappa_t = 1, \kappa_\lambda = 1) \sim |\mathcal{A}_1|^2 + 2\Re\mathcal{A}_1^* \mathcal{A}_2 + |\mathcal{A}_2|^2$$

$$\sigma(\kappa_t = 1, \kappa_\lambda = 20) \sim |\mathcal{A}_1|^2 + 2 \cdot 20\Re\mathcal{A}_1^* \mathcal{A}_2 + 20^2 |\mathcal{A}_2|^2$$

$$\begin{aligned} \sigma(\kappa_t, \kappa_\lambda) \sim \kappa_t^2 \left[\left(\kappa_t^2 + \frac{\kappa_\lambda^2}{20} - \frac{399}{380} \kappa_\lambda \kappa_t \right) |S(1, 0)|^2 + \left(\frac{40}{38} \kappa_\lambda \kappa_t - \frac{2}{38} \kappa_\lambda^2 \right) |S(1, 1)|^2 \right. \\ \left. + \left(\frac{\kappa_\lambda^2 - \kappa_\lambda \kappa_t}{380} \right) |S(1, 20)|^2 \right] \end{aligned}$$

HH summary



good sensitivity at low resonant masses